

Downregulation of microRNA-224-3p Hampers Retinoblastoma Progression via Activation of the Hippo-YAP Signaling Pathway by Increasing LATS2

Lili Song, Yanxia Huang, Xinli Zhang, Shaoping Han, Min Hou, and Hongxia Li

Department of Ophthalmology, Luoyang Central Hospital Affiliated to Zhengzhou University, Luoyang, P.R. China

Correspondence: Lili Song, Department of Ophthalmology, Luoyang Central Hospital Affiliated to Zhengzhou University, No. 288, Zhongzhou Middle Road, Luoyang 471009, Henan Province, P.R. China; prosong_lili@163.com.

Received: May 15, 2019

Accepted: December 22, 2019

Published: March 18, 2020

Citation: Song L, Huang Y, Zhang X, Han S, Hou M, Li H. Downregulation of microRNA-224-3p hampers retinoblastoma progression via activation of the Hippo-YAP signaling pathway by increasing LATS2. *Invest Ophthalmol Vis Sci.* 2020;61(3):32. <https://doi.org/10.1167/iovs.61.3.32>

PURPOSE. The pivotal role of microRNAs (miRNAs or miRs) has been proved in the pathogenesis of retinoblastoma. miR-224-3p is demonstrated to be involved in several tumors. However, the underlying mechanism of miR-224-3p in retinoblastoma is yet to be investigated. Therefore, this study was designed to identify the regulation of miR-224-3p in human retinoblastoma.

METHODS. The expression pattern of miR-224-3p and large tumor suppressor 2 (LATS2) in retinoblastoma was measured by reverse transcription quantitative polymerase chain reaction. Afterward, the interaction between miR-224-3p and LATS2 was identified using a dual luciferase reporter gene assay. Next, gain-of-function and loss-of-function approaches were employed to examine the effects of miR-224-3p and LATS2 as well as their interaction on cell apoptosis, proliferation and angiogenesis abilities, and tumorigenesis. Whether the Hippo-YAP signaling pathway was involved in tumorigenesis was analyzed by determining downstream genes.

RESULTS. LATS2 was downregulated in retinoblastoma, and its overexpression promoted apoptosis and suppressed proliferation of retinoblastoma cells. miR-224-3p, highly expressed in retinoblastoma, inhibited the expression of its target gene LATS2, which inhibited activation of the Hippo-YAP signaling pathway. Suppression of miR-224-3p promoted apoptosis while suppressing the proliferation of retinoblastoma cells and angiogenesis. Tumor progression induced by upregulation of miR-224-3p was diminished by restoration of LATS2. It was observed that tumor growth and angiogenesis were reduced by depleted miR-224-3p in the animal experiments.

CONCLUSIONS. The present study suggests that miR-224-3p targets LATS2 and blocks the Hippo-YAP signaling pathway activation, thus preventing the progression of retinoblastoma, which could be a new therapeutic target for retinoblastoma.

Keywords: microRNA-224-3p, large tumor suppressor 2, Hippo-YAP signaling pathway, retinoblastoma, apoptosis, angiogenesis

Retinoblastoma is an aggressive pediatric cancer originating from the retina that occurs either genetically in children or sporadically in adults.^{1,2} The clinical manifestations of retinoblastoma include leukocoria, strabismus, color change of the iris, enlargement of the cornea and eyes, noninfective orbital inflammation, and bulging of the eye from the orbit in very late-stage disease.³ The current treatment options for retinoblastoma include enucleation, radiation, focal techniques, and systemic chemotherapy as well as delivering chemotherapy to the eyes with less systemic exposure.⁴ Yet the genetic and epigenetic complexity of retinoblastoma is widely appreciated and evidenced by the intricate network of cellular and epigenetic components that modulate tumor progression. Recent evidence has suggested that epigenetic alterations are essential in the pathogenesis of retinoblastoma.⁵ Therefore, understanding the molecular

mechanism associated with the biology of retinoblastoma will be of great clinical value.

MicroRNAs (miRNAs or miRs) are small noncoding RNAs that modulate cellular and physiologic functions such as cell cycle, transcriptional activation or silencing, and cellular signaling transduction.⁶ It has been well documented that miRNAs are vital regulators in many cases of cancer playing dual roles as either tumor suppressors or oncogenes.⁷ Particularly, dysregulated miRNAs in retinoblastoma have been widely investigated. For instance, miR-124 and miR-34a act as tumor suppressors^{8,9} while miR-125b functions as a tumor promoter.¹⁰ The carcinogenic role of miR-224-3p has also been identified in human cancer. Although the involvement of miR-224-3p in the progression of retinoblastoma remains unknown, ectopic expression of miR-224-3p has been detected in high-risk human papillomavirus (HPV)-positive

cervical cancer cells, and its overexpression has been proven to inhibit autophagy in HPV-infected cells.¹¹

miRNAs can bind to the 3' untranslated region (3'UTR) of their target mRNAs through the seed region to repress their posttranscription levels, thus mediating various biological processes.¹² Based on the findings from the starBase and TargetScan databases, miR-224-3p is predicted to target large tumor suppressor 2 (LATS2). LATS2, also identified as a target gene of miR-492, has been suggested to suppress the growth and migration of retinoblastoma cells.¹³ Moreover, LATS2 is already known as one of the mammalian core kinase components of the Hippo signaling pathway.¹⁴ The Hippo core kinase cassette, composed of Mst1/2, LATS1/2, and two adaptors, Sav1 and Mob, has been found to be dysregulated in human cancers.¹⁵ The Hippo signaling pathway usually acts as an antioncogenic pathway in regulating tissue homeostasis wherein YAP and TAZ exert oncogenic roles in human cancers.¹⁶ Based on the aforementioned findings, we hypothesized that miR-224-3p might affect the progression of retinoblastoma by regulating LATS2 expression and the Hippo-YAP signaling pathway. Therefore, we conducted the present study to validate this hypothesis and provide further insight on the molecular mechanism associated with tumorigenesis in retinoblastoma.

MATERIALS AND METHODS

Ethics Statement

This study was performed with the approval of the Ethics Committee of Luoyang Central Hospital Affiliated to Zhengzhou University. Written informed consent was obtained from the guardians of all participants. All experimental procedures involving animals were performed in strict accordance with the Animal Care Committee (Luoyang Central Hospital Affiliated to Zhengzhou University, 201805004). Extensive efforts were made to ensure minimal suffering of the animals used during the study.

Microarray-Based Gene Expression Profiling and miRNA Prediction

Microarray profiles of retinoblastoma were obtained from the Gene Expression Omnibus (GEO) database (<https://www.ncbi.nlm.nih.gov/geo/>), and differentially expressed genes were analyzed using the “limma package” in R software with $|\log\text{Fold Change}| > 2$ and $P < 0.05$ used as the screening criteria. The top 300 miRNAs that might regulate LATS2 were selected from the starBase database (<http://starbase.sysu.edu.cn/mirMrna.php>), TargetScan database (http://www.targetscan.org/vert_71/), and miRmap database (<https://mirmap.ezlab.org/>). The intersection of all the aforementioned miRNAs was obtained at jvenn (<http://jvenn.toulouse.inra.fr/app/example.html>). The pathway involving the LATS2 gene was analyzed at the Kyoto Encyclopedia of Genes and Genomes (KEGG) database (<https://www.genome.jp/kegg/>).

Tissue Collection

Retinoblastoma tissues were collected from 67 patients with retinoblastoma who were diagnosed at the Luoyang Central Hospital Affiliated to Zhengzhou University from 2016 to 2017. All patients enrolled in this study had not received any therapy before the surgery. The patients were within the

ages of 9 months to 10 years, including 39 boys and 28 girls. All patients were diagnosed and conformed by pathologists. Normal retinal tissues were collected from corneal transplantation donors ($n = 15$) as normal controls. Tumor samples and nonneoplastic tissues were frozen in liquid nitrogen immediately after excision for RNA extraction.

Cell Culture

Human retinoblastoma cell line Y79 was obtained from the American Type Culture Collection (ATCC, Manassas, VA, USA). The cells were cultured in RPMI-1640 medium containing 10% (v/v) fetal bovine serum (FBS) (GIBCO BRL, Grand Island, NY, USA) and 1% (v/v) penicillin-streptomycin-glutamine (100×) (GIBCO BRL). The cell culture was performed in an incubator at 37°C with 5% CO₂ (Thermo Fisher Scientific, Waltham, MA, USA).

Cell Transfection

Prior to transfection, cell confluence was adjusted to 50% to 60%. The retinoblastoma cells were seeded into a 24-well plate and transfected according to the instructions of the Lipofectamine 2000 kit (Invitrogen, Carlsbad, CA, USA). The plasmids used for transfection included miR-224-3p mimic, miR-224-3p inhibitor, and LATS2 overexpression plasmid (oe-LATS2) or their negative controls (mimic-NC, inhibitor-NC, and oe-NC). The plasmids were all purchased from Dharmacon (Lafayette, CO, USA).

RNA Isolation and Quantitative RT-PCR (RT-qPCR)

Total RNA in tissues and cells was isolated using a Trizol Plus RNA Purification Kit (Invitrogen). The total RNA concentration was measured using a Nanodrop ND-1000 instrument (Nanodrop Technologies, Wilmington, DE, USA). Then, the cDNA was reversely transcribed using a large-capacity cDNA reverse transcription kit (Applied Biosystems, Foster City, CA, USA). The expression of miR-224-3p was determined using a mirVana qRT-PCR-miRNA detection kit (Applied Biosystems, Foster City). Glyceraldehyde-3-phosphate dehydrogenase and U6 small nuclear RNA (U6) were used as internal controls for mRNA and miRNA, respectively (Table 1). The relative expression was analyzed using the $2^{-\Delta\Delta\text{CT}}$ method.

Western Blot Analysis

Total protein was isolated from cells using radioimmunoprecipitation assay lysis buffer (Beyotime Biotechnology, Shanghai, China) supplemented with protease inhibitor (Roche, Basel, Switzerland). The concentration of total protein was quantified using a Bicinchoninic Acid Protein Assay Kit (Beyotime Biotechnology). The primary antibodies, including LATS2 (1 µg/mL, ab110780), B-cell lymphoma 2 (Bcl-2) (1:1000, ab32124), Bcl-2 associated X protein (Bax) (1:1000, ab3250), vascular endothelial growth factor (VEGF) (1:1000, ab32152), tafazzin (TAZ) (1 µg/mL, ab84927), Yes associated protein (YAP) (1:5000, ab52771), p-YAP (1:10000, ab76252), connective tissue growth factor (CTGF) (1:1000, ab6992), and cysteine rich angiogenic inducer 61 (CYR61) (1 µg/mL, ab24448), were purchased from Abcam, Inc. (Cambridge, UK) except p-TAZ (1:1000, sc-17610-R; Santa Cruz, USA). These primary antibodies were diluted with 1% BSA (Sigma-Aldrich, St. Louis, MO, USA). After the proteins

TABLE 1. Primer Sequences for RT-qPCR

Gene	Primer Sequence (5'-3')
miR-224-3p	Forward: TGATGTGGGTGCTGGTGTGTC Reserve: TTGTGTTGGGGCAGTACTG
LATS2	Forward: CTTTGGAACCGCGGCGT Reserve: TATCACTCTCTCCAGGGGCG
Bax	Forward: GGATGCGTCCACCAAGAAG Reserve: GCCTTGAGCACCAGTTTGC
Bcl-2	Forward: CACGCTGGGAGAACA Reserve: CTGGGAGGAGAAGATG
VEGF	Forward: CCAGCACATAGGAGAGATGAGCTT Reserve: TCTTTCTTTGGTCTGCATTACAT
TAZ	Forward: TGGACCAAGTACATGAACCACC Reserve: CTGGTGATTGGACACGGTGA
YAP	Forward: CGCTCTTCAACGCCGTCA Reserve: AGTACTGGCCTGTCGGGAGT
CTGF	Forward: AAACATTTCTGAGTTTTCTTGAGCA Reserve: TGTGGTGTGTATGCCTGCAA
CYR61	Forward: TCCTCTGTGTCCCAAGAAC Reserve: TTCAGGCTGCTGTACTACTGG
U6	Forward: CGCTTCGGCAGCACATATACTA Reserve: CGCTTCACGAATTTGCGTGTCA
GAPDH	Forward: TCATCTCTGCCCCCTCTGCTG Reserve: GCCTGCTCACCACCTTCTTG

GAPDH, glyceraldehyde-3-phosphate dehydrogenase.

were transferred to the polyvinylidene fluoride membrane, the membrane underwent incubation with the primary antibodies for 12 hours. After incubation with the second antibody, the protein signals were captured by adding 200 μ L Immobilon Western chemiluminescent horseradish peroxidase matrix (Merck Millipore, Billerica, MA, USA) in a Bio-Rad ChemiDoc XRS system (Bio-Rad, Hercules, CA, USA) to the membrane surface, and the intensity of the bands was quantified with the use of an Image Lab software (BioRad).

Dual Luciferase Reporter Gene Assay

The binding site analysis between miR-224-3p and LATS2 was determined using a biological prediction website, from which the fragment sequence containing the site of action was obtained. The 3'UTR of LATS2 was cloned and amplified into the luciferase vector pmirGLO (E1330; Promega, Madison, WI, USA), designated as pLATS2 wide type (Wt). The pLATS2-mutant (Mut) vector was constructed using site-directed mutagenesis. The pRL-TK vector expressing *Renilla* luciferase (E2241; Promega) was used as internal reference. The NC and miR-224-3p mimic were cotransfected into Y79 cells with the recombinant luciferase reporter vector. The fluorescence intensity at 560 nm (firefly relative light unit [RLU]) and 465 nm (*Renilla* RLU) was measured using the Dual Luciferase Reporter Gene Assay Kit (GM-040502A; Qcbio S&T, Shanghai, China). The ratio of the firefly RLU to *Renilla* RLU was regarded as the relative luciferase activity.

5-Ethynyl-2'-Deoxyuridine (EdU) Assay for Cellular Proliferation

Y79 cells in logarithmic growth phase were seeded into a 24-well plate at 1×10^4 cells per well and cultured in an incubator. The culture medium was added with EdU at a final concentration of 100 μ M/L. After 48 hours of incu-

bation, fluorescence staining was performed in accordance with the manufacturer's protocol of the EdU kit (C10310; Ribo Co., Ltd., Guangzhou, Guangdong, China). Images were obtained using an Olympus microscope (BX53; Olympus, Tokyo, Japan).

Flow Cytometry

Apoptosis was assessed by annexin V/propidium iodide (PI) double staining. Y79 cells received treatment with 0.25% trypsin, and they were suspended and seeded into a culture plate at a density of 1×10^5 cells/mL, followed by three washes with PBS precooled at 4°C and trypsinization. After centrifugation at 290 g for 5 minutes, the supernatant was removed and the cells were resuspended in PBS again. The supernatant was discarded by centrifuging the 100- μ L cell suspension (1×10^6 cells/mL) at 290 g for 5 minutes. Then, the cells were mixed with 500 μ L $1 \times$ binding buffer, 5 μ L FITC-labeled annexin V-FITC, and 10 μ L PI in succession. The mixture underwent incubation with a flow cytometer (BDLSR II; BD Biosciences, San Jose, CA, USA) at room temperature for 5 to 10 minutes under dark conditions, followed by apoptosis analysis.

After centrifugation of the 100- μ L cell suspension at 290 g for 5 minutes, the supernatant was discarded. The sample was washed twice with precooled 200 μ L PBS, treated with 20 μ L RNase for 30 minutes at 37°C, and cultured on ice for 15 minutes with 400 μ L PI (C0080; Solarbio, Beijing, China) in the absence of light. Finally, cell cycle was examined by a flow cytometer (BDLSR II; BD Biosciences) at 488 nm.

Endothelial Cell Tube Formation Assay

Tube formation was observed in human umbilical vein endothelial cells (HUVECs) (354151; Corning Incorporated, New York, NY, USA) to evaluate angiogenesis. HUVECs and Y79 cells were cultured in Dulbecco's modified Eagle's

medium (DMEM) containing 10% FBS and L-15 medium, respectively, in an incubator at 37°C. The Y79 cells were transfected, and the supernatant was collected 48 hours later. The cell debris was removed by centrifugation under aseptic conditions, and the tumor cell culture supernatant was obtained. Tumor conditioned medium was prepared using the mixture of tumor supernatant, DMEM, and FBS (4:5:1). Subsequently, each well in a 96-well plate was added with 50 μ L Matrigel and allowed to polymerize in an incubator at 37°C for 30 minutes. HUVEC suspension was cultured with the prepared tumor conditioned medium at 37°C with 5% CO₂ for 8 hours. Three replicates were set for each group. Afterward, four fields were randomly selected per well under phase contrast microscope, and the number of tubules was counted.

Xenograft Tumor in Nude Mice

The Y79 cells were transfected with NC mimic, miR-224-3p mimic, NC inhibitor, or miR-224-3p inhibitor, respectively. A total of 40 BALB/C nude mice (weighting 19–23 g; aged 7 weeks) purchased from Zhengzhou University Experimental Animal Center (Zhengzhou, China) were injected with Y79 cell suspension in 0.2 mL PBS into the left side. The mice were housed in a standard laboratory environment and maintained on a 12-hour light-dark cycle at 21°C with free access to water and food. Tumor volume (V) was calculated with the long diameter (L) measured by vernier caliper using the following formula: $V = 1/2 (L/2)^2$. The mice were euthanized 4 weeks after the injection. The tumor weight and tumor volume were measured.

Immunohistochemistry (IHC)

The tissue specimen was fixed in formalin, embedded with paraffin, sectioned at a thickness of 5 μ m, and dehydrated with alcohol of gradient concentrations. Antigen retrieval was performed for 20 minutes in 10 mM citrate buffer (pH 6) containing 0.05% polysorbate and 98 ester. In accordance with the instructions provided on the IHC kit (Invitrogen), the tissues were treated with 3% H₂O₂ and Zymed solution A (Zymed Laboratories, San Francisco, CA, USA) for 10 minutes and underwent incubation with primary antibody to VEGF (1:250, ab32152; Abcam, Inc.) or CD31 (1:50, ab28364; Abcam, Inc.) at room temperature for 1 hour. The tissues were exposed to Zymed solutions B and C for 10 minutes each, in which 3,3-diaminobenzidine (DAKO, Glostrup, Denmark) was used as chromogen for 5 minutes. The tissues were counterstained with hematoxylin (Thermo Fisher Scientific) at room temperature for 2 minutes at a ratio of 1:17 and immersed in 1% ammonium hydroxide at room temperature for 1 minute. Citrate buffer was considered the NC for staining instead of primary antibody. Images were obtained using an Olympus DP70 microscope.

Statistical Analysis

The Statistic Package for Social Science (SPSS) 21.0 statistical software (IBM Corp., Armonk, NY, USA) was used for statistical analysis. The measurement data were expressed as mean \pm standard deviation. The comparison of paired data following normal distribution and homogeneity of variance between two groups was conducted by a paired *t* test, while that of unpaired data between two groups was conducted using an unpaired *t* test. Data among multiple groups were

compared using 1-way ANOVA, followed by Tukey's post hoc test. Data comparison within one group at different time points was performed by repeated-measures ANOVA, followed by Bonferroni's post hoc test. $P < 0.05$ was considered statistically significant.

RESULTS

LATS2 Is Poorly Expressed in Retinoblastoma Tissues and Cells

Retinoblastoma gene expression data set GSE111168 was retrieved from the GEO database, which consisted of three normal samples and three retinoblastoma samples, followed by differential analysis on gene expression. The expression of LATS2 was significantly reduced in retinoblastoma samples in comparison with para-tumor samples according to GSE111168 (Fig. 1A). Consistently, the results from the RT-qPCR revealed a lower expression of LATS2 in retinoblastoma tissues than that in normal retinal tissues ($P < 0.05$) (Fig. 1B). Western blot analysis showed (Fig. 1C) that the protein level of LATS2 in retinoblastoma tissues was markedly lower than that in normal retinal tissues ($P < 0.05$). The aforementioned findings indicated that LATS2 was poorly expressed in retinoblastoma.

Overexpression of LATS2 Promotes Apoptosis and Inhibits Proliferation and Angiogenesis of Retinoblastoma Cells

With results learning the downregulation of LATS2 in retinoblastoma, next focus was shifted to the possible effects of LATS2 on retinoblastoma cell biological behaviors. Y79 cells were transfected with oe-LATS2 with oe-NC as control, and then RT-qPCR and Western blot analysis were performed to determine the transfection efficiency. The results showed that the mRNA and protein levels of LATS2 were increased in Y79 cells following transfection with oe-LATS2 ($P < 0.05$) (Figs. 2A, 2B). Next, the result of the EdU assay showed that Y79 cells transfected with oe-LATS2 presented with attenuated proliferation ability compared with that of Y79 cells transfected with oe-NC ($P < 0.05$) (Fig. 2C). The flow cytometric data showed that oe-LATS2 transfection resulted in more G0/G1 phase-arrested Y79 cells and fewer S phase-arrested Y79 cells than oe-NC transfection ($P < 0.05$) (Fig. 2D). Compared with the Y79 cells transfected with oe-NC, Y79 cells transfected with oe-LATS2 had an increased apoptosis rate ($P < 0.05$) (Fig. 2E). The functional significance of LATS2 in tumor angiogenesis was evaluated using HUVEC tube formation induced by conditioned medium, the results of which showed that overexpression of LATS2 resulted in the inhibition of angiogenesis ($P < 0.05$) (Fig. 2F). The protein levels of antiapoptotic factor Bcl-2 and apoptotic factor Bax, as well as angiogenic factor VEGF in Y79 cells, were measured by Western blot analysis, which showed decreased protein levels of VEGF and Bcl-2 and increased Bax protein level in Y79 cells after transfection with oe-LATS2 ($P < 0.05$) (Fig. 2G). These findings demonstrated that elevated LATS2 promoted cell apoptosis in retinoblastoma and inhibited cell proliferation and angiogenesis.

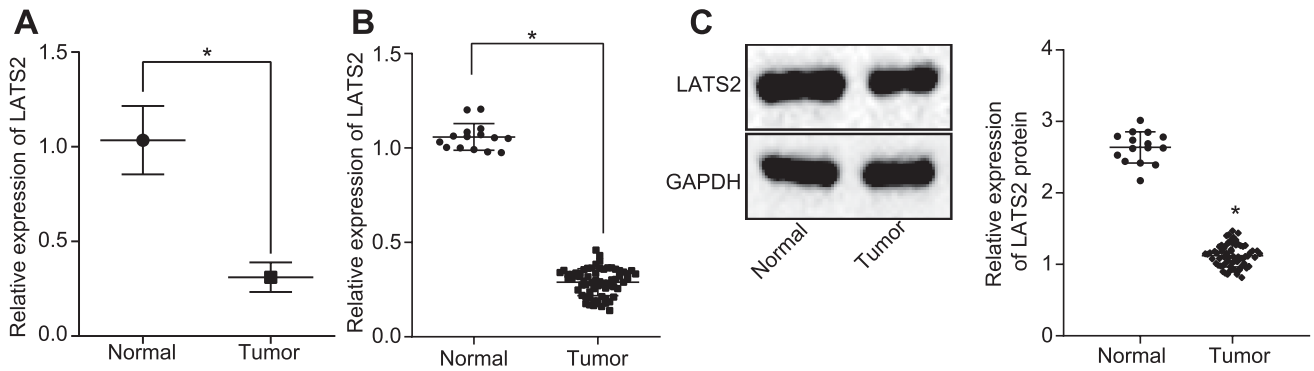


FIGURE 1. Downregulation of LATS2 is found in retinoblastoma tissues and cells. **(A)** Expression of LATS2 in GSE111168. **(B)** Expression of LATS2 in retinoblastoma tissues ($n = 67$) and normal retinal tissues ($n = 15$) determined by RT-qPCR. **(C)** Protein level of LATS2 in retinoblastoma tissues ($n = 67$) and normal retinal tissues ($n = 15$) normalized to glyceraldehyde-3-phosphate dehydrogenase (GAPDH) determined by Western blot analysis ($n = 67$). $*P < 0.05$ versus the normal tissue. Data expressed by mean \pm standard deviation between tumor and normal retinal tissues were compared using paired t test and those between the other two groups were compared using the independent sample t test. The cell experiment was repeated three times independently.

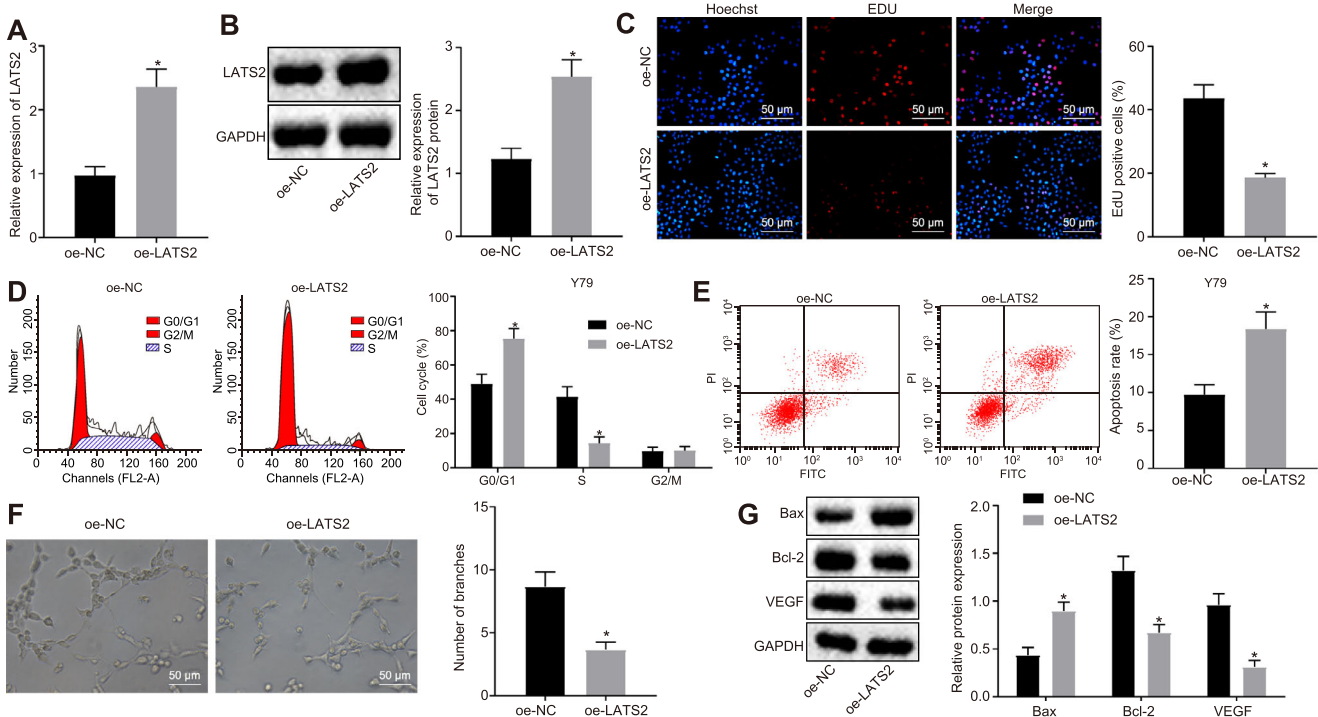


FIGURE 2. Overexpression of LATS2 promotes apoptosis while inhibiting proliferation and angiogenesis of Y79 cells. **(A)** Expression of LATS2 determined by RT-qPCR in the transfected cell lines. **(B)** Protein level of LATS2 in cells normalized to GAPDH determined by Western blot analysis. **(C)** Cell proliferation determined by EdU assay ($\times 200$, scale bar: 50 μm). **(D)** Cell cycle distribution identified by flow cytometry. **(E)** Cell apoptosis detected by flow cytometry. **(F)** Angiogenesis measured by tube formation assay ($\times 200$, scale bar: 50 μm). **(G)** Protein levels of Bax, Bcl-2, and VEGF normalized to GAPDH in cells measured by Western blot analysis. $*P < 0.05$ versus Y79 cells transfected with oe-NC; data expressed by mean \pm standard deviation between two groups were compared using independent sample t test. The cell experiment was repeated three times independently.

miR-224-3p Specifically Targets LATS2

The miRNAs that could regulate LATS2 were predicted from starBase, TargetScan, and miRmap databases, with 13 miRNAs in the intersection (Table 2, Fig. 3A). The expression of 13 miRNAs in retinoblastoma was determined by RT-qPCR, and the expression of miR-224-3p was found to be highly expressed in retinoblastoma tissues with a largest fold change compared with normal retinal tissues (Fig. 3B). To

investigate the relationship between miR-224-3p and LATS2 in retinoblastoma cells, the presence of miR-224-3p binding sites in LATS2 mRNA was analyzed by the TargetScan analysis (Fig. 3C). Next, the results of the dual luciferase reporter gene assay indicated that the luciferase activity of the LATS2-Wt 3'UTR was suppressed by miR-224-3p mimic transfection ($P < 0.05$), whereas that of the LATS2-Mut 3'UTR was not affected ($P > 0.05$) (Fig. 3D). Then, we upregulated the expression of miR-224-3p by transfection with miR-224-

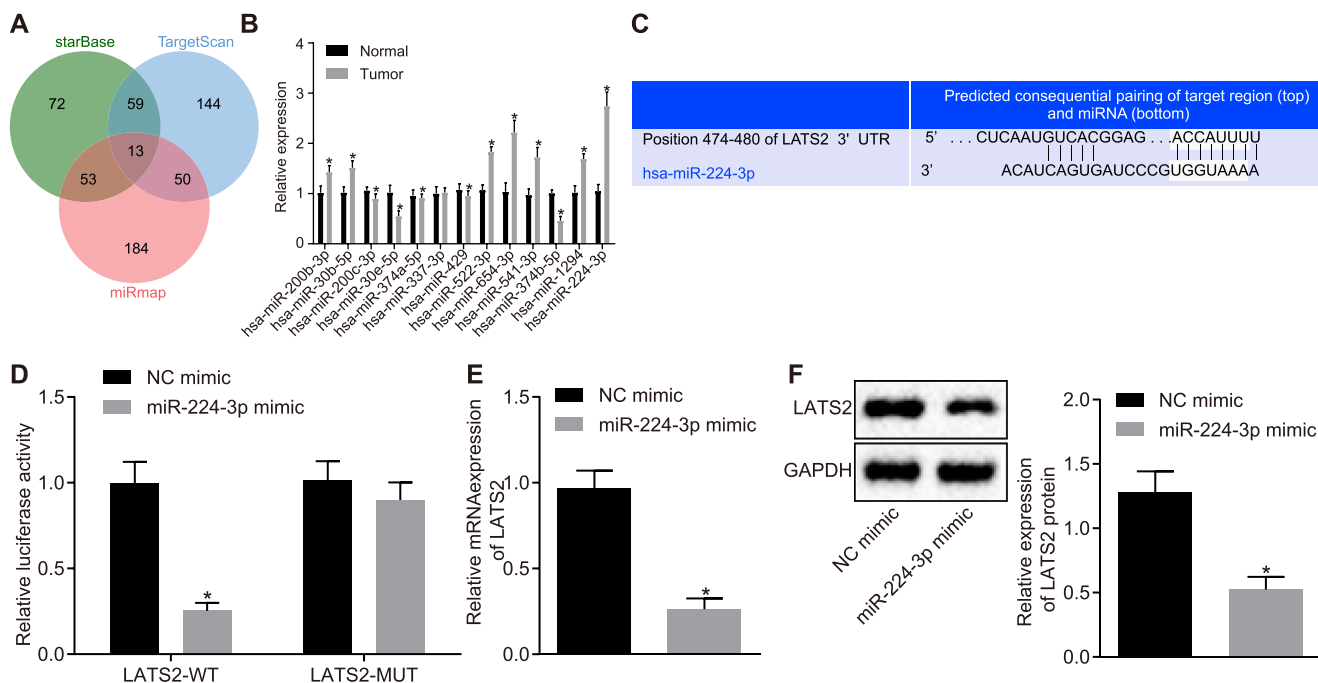


FIGURE 3. LATS2 is a target gene of miR-224-3p. (A) Predicted miRNAs that regulated LATS2. Three circles represented the predicted results using three databases (starBase, TargetScan, and miRmap), and the middle part represented the intersection of the predicted results from three databases. (B) Expression of 13 miRNAs in retinoblastoma tissues ($n = 67$) and normal retinal tissues ($n = 15$) determined by RT-qPCR. (C) Binding site between miR-224-3p and LATS2 predicted on TargetScan. (D) Relative luciferase activity of LATS2-Wt and LATS2-Mut in the presence of miR-224-3p. (E) The mRNA expression of LATS2 after upregulation of miR-224-3p determined by RT-qPCR. (F) Protein levels of LATS2 normalized to GAPDH after upregulation of miR-224-3p measured by Western blot analysis. $*P < 0.05$ versus the normal tissue or the Y79 cells transfected with NC mimic. Data expressed by mean \pm standard deviation between tumor and normal retinal tissues were compared using paired t test while those between other two groups were performed using the independent sample t test. The cell experiment was repeated three times independently.

TABLE 2. Intersected miRNAs Among the Predicted miRNAs from starBase, TargetScan, and miRmap

starBase TargetScan miRmap
hsa-miR-200b-3p
hsa-miR-30b-5p
hsa-miR-200c-3p
hsa-miR-30e-5p
hsa-miR-374a-5p
hsa-miR-337-3p
hsa-miR-429
hsa-miR-522-3p
hsa-miR-654-3p
hsa-miR-541-3p
hsa-miR-374b-5p
hsa-miR-1294
hsa-miR-224-3p

miR, microRNA.

3p mimic with NC mimic as the control and determined the expression of LATS2 following transfection using RT-qPCR and Western blot analysis, which revealed a reduction in mRNA and protein expression of LATS2 in the presence of miR-224-3p mimic ($P < 0.05$) (Figs. 3E, 3F). Therefore, miR-224-3p specifically binds to the 3'UTR of LATS2 mRNA and downregulates LATS2 expression.

miR-224-3p Promotes the Proliferation and Cell Cycle Progression of Retinoblastoma Cells by Targeting LATS2

To investigate the expression pattern of miR-224-3p in retinoblastoma, the expression of miR-224-3p in 67 retinoblastoma tissues and normal retinal tissues was measured by RT-qPCR. The expression of miR-224-3p in retinoblastoma tissues was higher than that in normal retinal tissues ($P < 0.05$) (Fig. 4A).

To explore the regulatory role of miR-224-3p in retinoblastoma progression, miR-224-3p expression was altered by transfection with miR-224-3p mimic or miR-224-3p inhibitor, with NC mimic or NC inhibitor used as respective controls. RT-qPCR results showed that miR-224-3p mimic transfection upregulated the expression of miR-224-3p, while miR-224-3p inhibitor transfection lowered the expression of miR-224-3p ($P < 0.05$) (Fig. 4B).

Cell proliferation following transfection was measured by the EdU assay, which showed enhanced cell proliferation following transfection with miR-224-3p mimic while it was diminished by transfection with miR-224-3p inhibitor ($P < 0.05$). In addition, cotransfection with miR-224-3p mimic and oe-LATS2 resulted in decreased cell proliferation compared with cotransfection with miR-224-3p mimic and oe-NC ($P < 0.05$) (Fig. 4C). The results from flow cytometry (Fig. 4D) depicted more G0/G1 phase-arrested cells yet fewer S phase-arrested cells caused by transfection with miR-224-3p mimic ($P < 0.05$). On the contrary, more G0/G1 phase-arrested

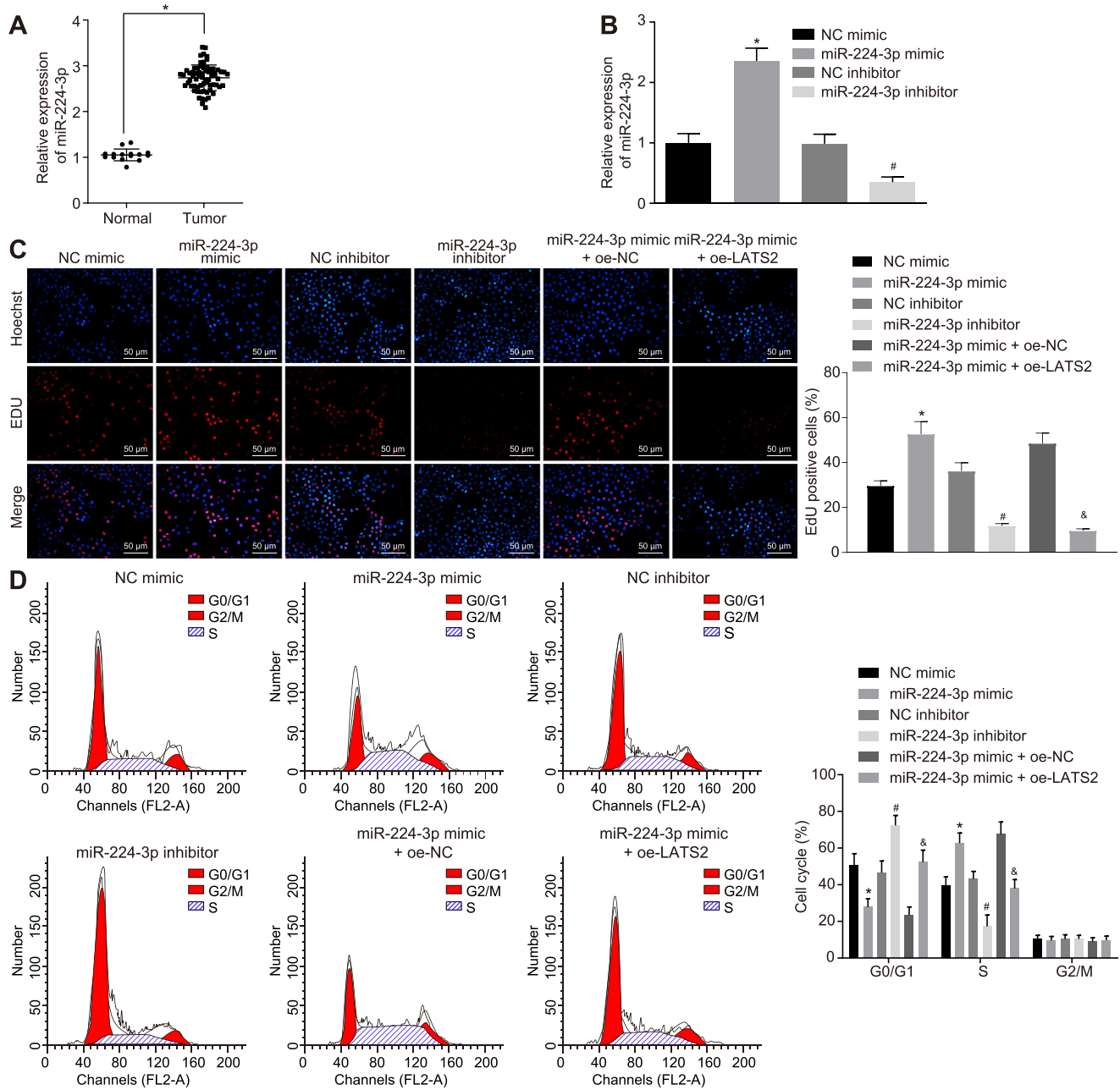


FIGURE 4. Upregulation of miR-224-3p leads to increased Y79 cell proliferation and cycle progression via inhibiting LATS2. **(A)** Expression of miR-224-3p in retinoblastoma tissues ($n = 67$) and normal retinal tissues ($n = 15$) determined by RT-qPCR. **(B)** Expression of miR-224-3p following transfection with miR-224-3p mimic or miR-224-3p inhibitor determined by RT-qPCR. **(C)** Proliferation ability of cells assessed by EdU assay ($\times 200$, scale bar: 50 μm). **(D)** Cell cycle distribution assessed by flow cytometry. * $P < 0.05$ versus the Y79 cells transfected with NC mimic; # $P < 0.05$ versus the Y79 cells transfected with NC inhibitor; & $P < 0.05$ versus the Y79 cells cotransfected with miR-224-3p mimic and oe-NC. Data expressed by mean \pm standard deviation between tumor and normal retinal tissues were compared using paired t test and those between the other two groups were analyzed using the independent sample t test. Comparisons among multiple groups were analyzed using 1-way ANOVA, followed by Tukey's post hoc test. The experiment was repeated three times independently.

cells yet fewer S phase-arrested cells were observed upon transfection with miR-224-3p inhibitor ($P < 0.05$). The cell cycle progression induced by miR-224-3p was repressed by restoration of LATS2 ($P < 0.05$). These findings suggest that miR-224-3p can stimulate the proliferation and cell cycle progression of retinoblastoma cells by targeting LATS2.

miR-224-3p Represses Cell Apoptosis While Promoting Angiogenesis by Targeting LATS2

The effect of miR-224-3p and LATS2 on apoptosis and angiogenesis of retinoblastoma cells was investigated. Flow cytometric data revealed a decline in cell apoptosis rate upon

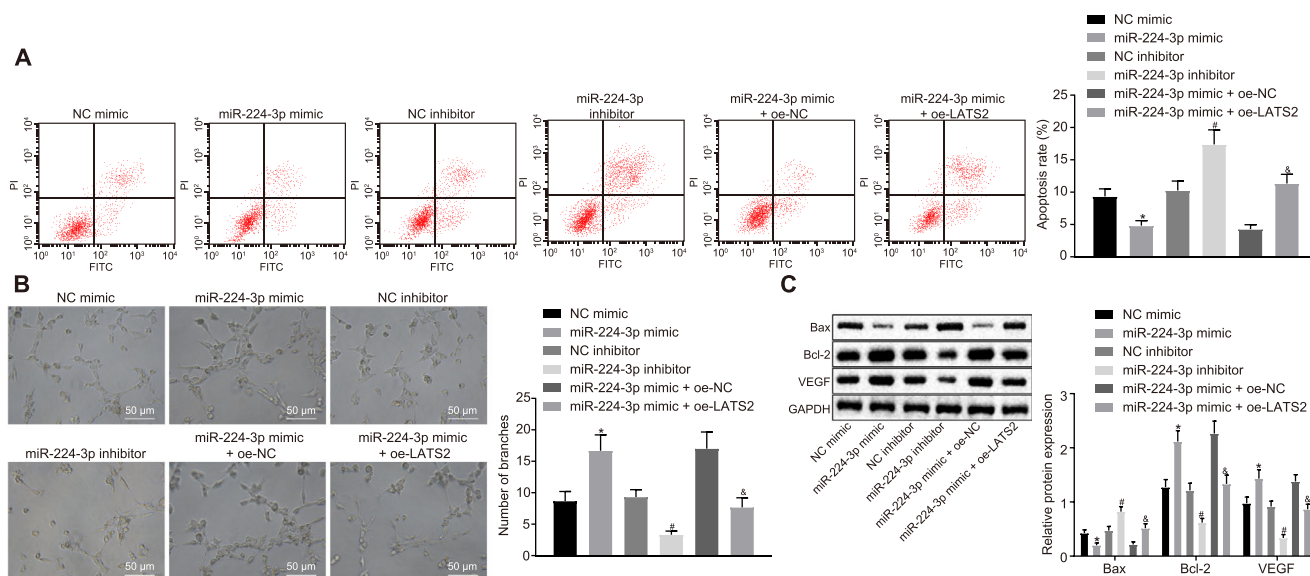


FIGURE 5. Upregulation of miR-224-3p leads to accelerated angiogenesis yet reduced Y79 cell apoptosis through downregulation of LATS2. (A) Apoptosis ability of cells assessed by flow cytometry. (B) Angiogenesis evaluated by tube formation assay ($\times 200$, scale bar: 50 μm). (C) Protein expression of Bax, Bcl-2, and VEGF normalized to GAPDH determined by Western blot analysis. * $P < 0.05$ versus the Y79 cells transfected with NC mimic; $^{\#}P < 0.05$ versus the Y79 cells transfected with NC inhibitor; $^{\&}P < 0.05$ versus the Y79 cells cotransfected with miR-224-3p mimic and oe-NC. Data expressed by mean \pm standard deviation between two groups were analyzed using independent sample t test. Comparisons among multiple groups were analyzed using 1-way ANOVA, followed by Tukey's post hoc test. The experiment was repeated three times independently.

transfection with miR-224-3p mimic but increased cell apoptosis caused by miR-224-3p inhibitor transfection compared with transfection with their corresponding NCs ($P < 0.05$). The cell apoptosis inhibited by miR-224-3p mimic was reversed following additional transfection with oe-LATS2 ($P < 0.05$) (Fig. 5A). As depicted in Figure 5B, angiogenesis was enhanced following transfection of miR-224-3p mimic while it was reduced in miR-224-3p inhibitor-transfected cells ($P < 0.05$). However, the promotive effects of miR-224-3p on angiogenesis induced by miR-224-3p mimic were diminished in response to LATS2 overexpression (all $P < 0.05$). Subsequently, cellular apoptosis and angiogenesis were evaluated following gain or loss function of miR-224-3p by measuring protein levels of VEGF, Bax, and Bcl-2. The Western blot analysis results (Fig. 5C) illustrated that the cells transfected with miR-224-3p mimic had increased protein levels of VEGF and Bcl-2 and decreased protein levels of Bax; however, cells transfected with miR-224-3p inhibitor presented with reduced VEGF and Bcl-2 protein levels and elevated protein levels of Bax (all $P < 0.05$). Compared with cotransfection with miR-224-3p mimic and oe-NC, cotransfection with miR-224-3p mimic and oe-LATS2 resulted in decreased protein expression of VEGF and Bcl-2 and increased protein expression of Bax ($P < 0.05$) (Fig. 5D). The aforementioned results highlighted that miR-224-3p promoted cell proliferation and angiogenesis while inhibiting apoptosis via downregulation of LATS2.

miR-224-3p Inhibits LATS2 and Further Blocks the Hippo-Yap Signaling Pathway

Subsequently, the underlying regulatory mechanisms were explored. Analysis of the KEGG metabolic pathway revealed that LATS2 was mainly involved in Hippo-YAP signaling

pathway (Fig. 6A). To investigate the effect of miR-224-3p on the Hippo-YAP signaling pathway, we first determined the mRNA expression of TAZ, YAP, CTGF, and CYR61 by RT-qPCR, which showed that the upregulation of miR-224-3p resulted in a higher expression of TAZ, YAP, CTGF, and CYR61, and a lower expression of TAZ, YAP, CTGF, and CYR61 was observed following the inhibition of miR-224-3p ($P < 0.05$) (Fig. 6B). Further determination was made regarding the protein expression measured by Western blot analysis. The results showed that upregulation of miR-224-3p increased protein expression of TAZ, YAP, CTGF, and CYR61, and the extents of TAZ and YAP phosphorylation significantly decreased, while inhibition of miR-224-3p led to reduced expression of TAZ, YAP, CTGF, and CYR61 and elevated extents of TAZ and YAP phosphorylation ($P < 0.05$) (Fig. 6C). Meanwhile, overexpression of LATS2 led to reduced expression of TAZ, YAP, CTGF, and CYR61 and elevated extents of TAZ and YAP phosphorylation ($P < 0.05$). LATS2 overexpression reversed the changes in expression of TAZ, YAP, CTGF, and CYR61 as well as extents of TAZ and YAP phosphorylation induced by enhancement of miR-224-3p ($P < 0.05$) (Figs. 6D, 6E). Therefore, miR-224-3p negatively regulates LATS2 and further blocks the Hippo-YAP signaling pathway.

Downregulation of miR-224-3p Suppresses Tumor Growth and Angiogenesis In Vivo

Last, tumor-bearing mice were employed to investigate the effects of miR-224-3p on retinoblastoma tumorigenesis in vivo. Y79 cells transfected with miR-224-3p mimic or miR-224-3p inhibitor were injected into nude mice, with cells transfected with NC mimic or NC inhibitor employed as the controls. Results showed that the volume of the formed

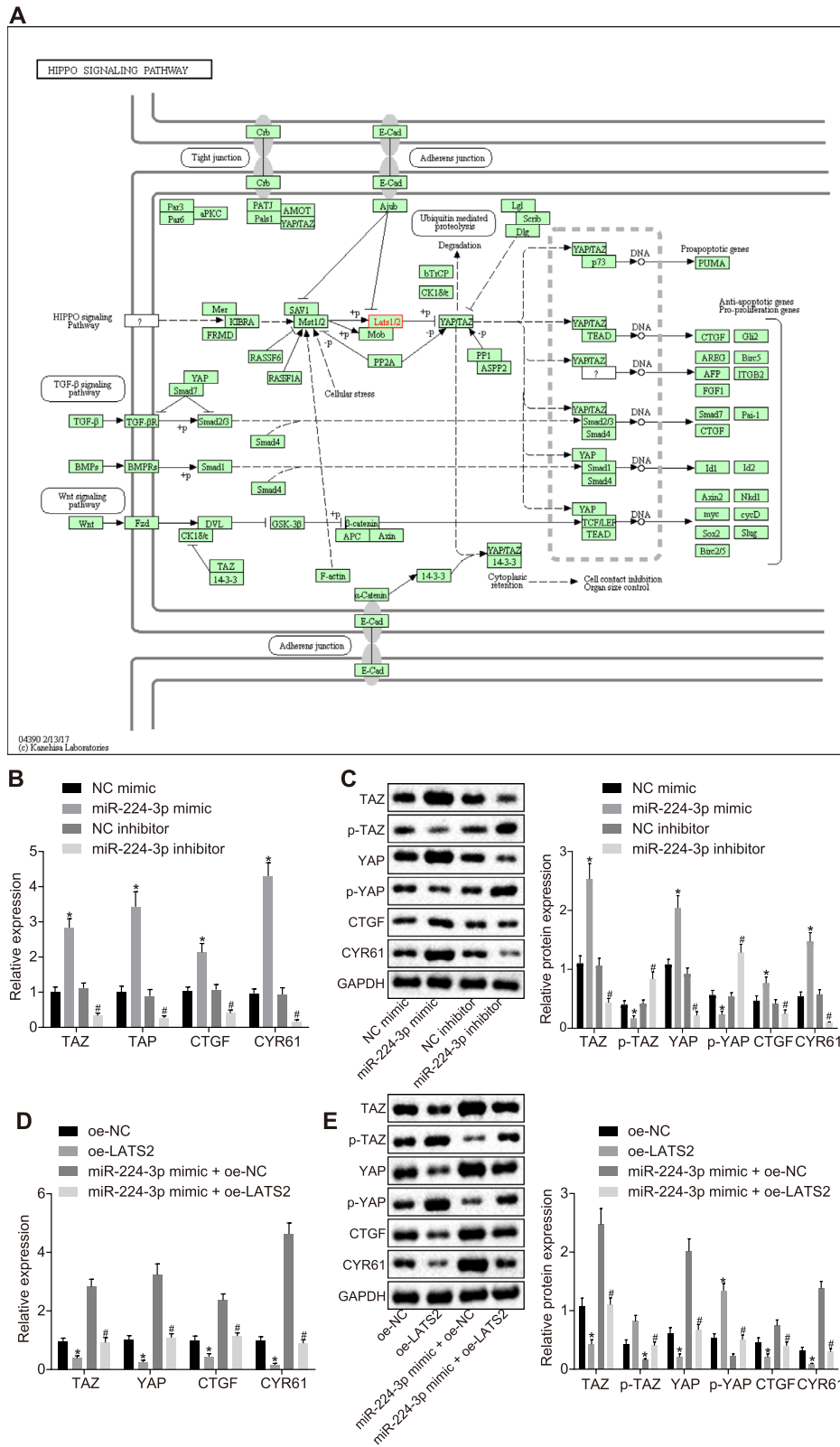


FIGURE 6. miR-224-3p inhibits the Hippo-YAP signaling pathway by downregulating expression of LATS2. **(A)** Involvement of LATS2 in the Hippo-YAP signaling pathway analyzed on KEGG. **(B)** mRNA expression of TAZ and YAP in cells determined by PT-qPCR. **(C)** Protein expression of TAZ, YAP, p-TAZ, and p-YAP in cells normalized to GAPDH determined by Western blot analysis. **(D)** mRNA expression of TAZ, YAP, CTGF, and CYR61 in cells determined by PT-qPCR. **(E)** Protein expression of TAZ, YAP, CTGF, CYR61, p-TAZ, and p-YAP in cells normalized to GAPDH determined by Western blot analysis. * $P < 0.05$ versus Y79 cells transfected with NC mimic or oe-NC; # $P < 0.05$ versus Y79 cells transfected with NC inhibitor or cotransfected with miR-224-3p mimic and oe-NC. Data expressed by mean \pm standard deviation among multiple groups were analyzed using 1-way ANOVA, followed by Tukey's post hoc test. The experiment was repeated three times independently.

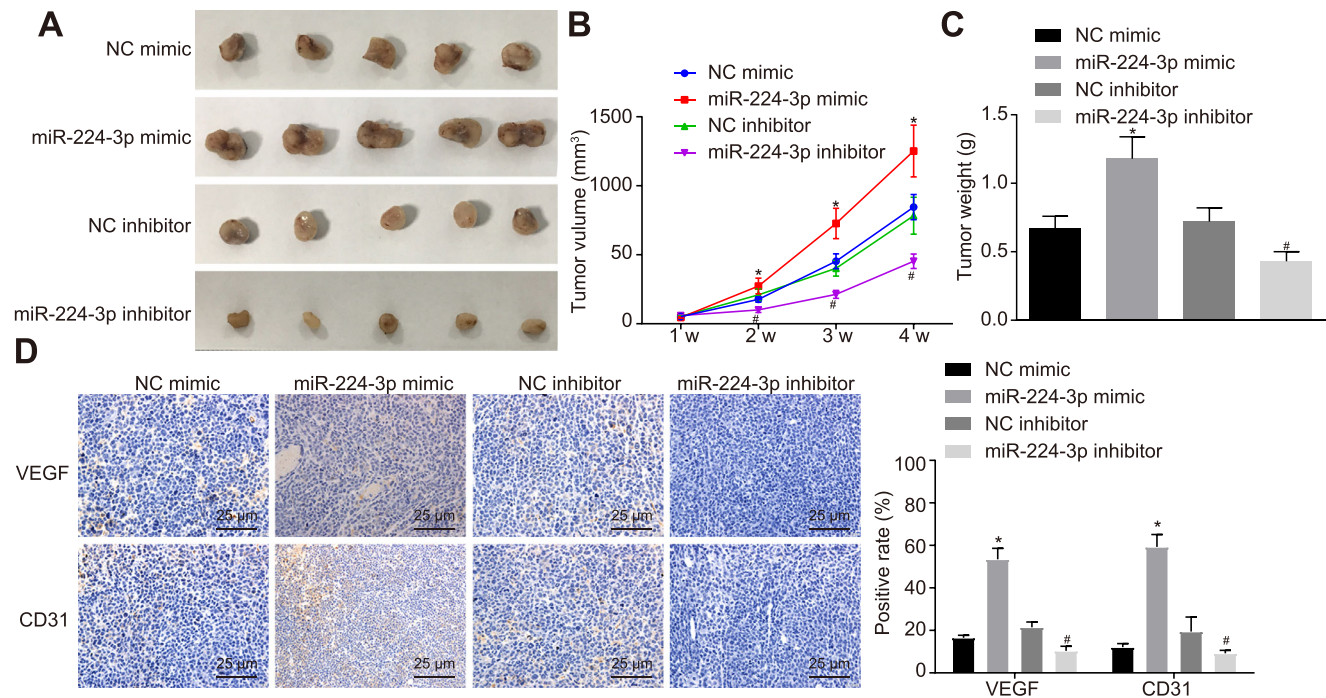


FIGURE 7. Downregulated miR-224-3p prohibits tumor growth and angiogenesis in nude mice. **(A)** Representative images of xenograft tumors in nude mice. **(B)** Tumor volume in nude mice. **(C)** Tumor weight in nude mice. **(D)** Positive expression of VEGF and CD31 detected by immunohistochemical staining ($\times 400$). * $P < 0.05$ versus the NC mimic group (nude mice bearing tumor in the presence of NC mimic); # $P < 0.05$ versus the NC inhibitor group (nude mice bearing tumor in the presence of NC inhibitor). Data expressed by mean \pm standard deviation among multiple groups were analyzed by 1-way ANOVA, followed by Tukey's post hoc test. The data among multiple groups at different time points were analyzed by repeated-measures ANOVA, followed by Bonferroni post hoc test, $n = 10$.

tumors was reduced by inhibition of miR-224-3p to varying degrees. On the contrary, the tumors maintained a good growth state and showed a gradual increase in volume in the presence of miR-224-3p ($P < 0.05$) (Figs. 7A–7C).

IHC detection of positive expression of angiogenic factors VEGF and CD31 showed a high expression in VEGF and CD31 in retinoblastoma tissues. VEGF-positive cells were mainly localized in the cytoplasm of tumor cells, strong positive-stained tumor cells were mostly localized in the anterior margin of tumor infiltration, and the CD31-positive cells were mainly localized in the cytoplasm. The positive expression of VEGF and CD31 was elevated in nude mice transplanted with miR-224-3p mimic-transfected Y79 cells, while it was lowered in nude mice transplanted with miR-224-3p inhibitor-transfected Y79 cells ($P < 0.05$) (Fig. 7D). The above results validated the protective role of downregulated miR-224-3p against retinoblastoma in vivo.

DISCUSSION

Retinoblastoma is the most common intraocular malignancy occurring during childhood, and 40% of retinoblastoma is caused by heredity and develops due to germline RB1 gene mutations.¹⁷ Although noncoding RNAs have been identified to participate in multiple types of cancers, their association with retinoblastoma was not identified until recently. miRNAs play a role as gene expression mediators, thereby modulating downstream signaling pathways and further affecting tumorigenesis and progression.¹⁸ However, the downstream mechanism of miR-224-3p in retinoblastoma cells requires further investigation. In the present study, miR-224-3p was found to inhibit LATS2 and to block the Hippo-

YAP signaling pathway, thus promoting the progression of retinoblastoma (Fig. 8). Therefore, our study highlighted the molecular mechanism and the promising therapeutic targets for retinoblastoma.

This study revealed miR-224-3p was highly expressed in retinoblastoma cells and involved in the progression of retinoblastoma. In cervical cancer, miR-224-3p has been proven to play a tumor promoter role.¹¹ Other miRNAs have been determined to play a similar role as miR-224-3p in retinoblastoma. For example, there is a high expression in miR-21 in retinoblastoma tissues, which is a carcinogenic miRNA, and the inhibition of miR-21 promotes apoptosis of cancer cells and suppresses cell proliferative potential.¹⁹ To explore the function of miR-224-3p in retinoblastoma, its expression was inhibited in retinoblastoma cells, the results of which revealed that miR-224-3p inhibition resulted in low expression of VEGF and suppressed angiogenesis. Angiogenesis, the formation of new blood vessels, is essential in providing oxygen and nutrient supply for tumor growth, as well as plays a key role in regulating other aspects such as tumor dissemination and metastasis.²⁰ A previous study suggested that miRNAs can regulate the angiogenic signals by targeting angiogenic factors and protein kinases.²¹ It has also been proven that miRNAs such as miR-150 could promote angiogenesis through upregulating VEGF.²² It is known that VEGF plays an angiogenic role and, therefore, has been linked to tumorigenesis, while the Bcl-2 gene has an antitumor effect.²³ Moreover, Bax protein is commonly known as a proapoptotic protein due to its ability to regulate mitochondria-dependent apoptosis.²⁴ In the present study, the inhibition of miR-224-3p resulted in the low expression of Bcl-2 protein and high expression of Bax protein, which

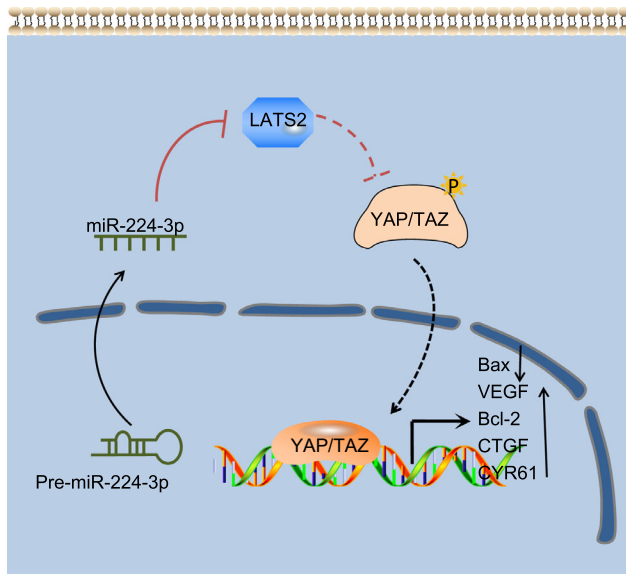


FIGURE 8. A mechanism map depicting the role of the miR-224-3p/LATS2/Hippo-YAP axis in the progression of retinoblastoma. miR-224-3p targets and negatively regulates LATS2 to inhibit the YAP/TAZ phosphorylation, whereby the Hippo signaling pathway activation is inhibited; following that, the downstream genes CTGF and CYR61 are upregulated, by which the apoptosis of retinoblastoma cells is suppressed while proliferation and angiogenesis are promoted.

was consistent with the finding that inhibited miR-224-3p resulted in the enhancement of apoptosis and suppression of proliferation of retinoblastoma cells. Therefore, the downregulation of miR-224-3p in retinoblastoma cells was found to have the potential to play an inhibitory role in relation to tumor progression. Moreover, tumor growth of nude mice was inhibited following the injection of miR-224-3p inhibitor-transfected retinoblastoma cells, indicating the antitumor effect exerted by miR-224-3p inhibition.

In the current study, it was observed that miR-224-3p could downregulate the expression of LATS2 and further block the activation of the Hippo-YAP signaling pathway, ultimately resulting in the advanced progression of retinoblastoma and promotion of angiogenesis. LATS2 was identified as a target gene of miR-224-3p in this study. Studies have shown that there is a relationship between LATS2 and the progression of retinoblastoma.^{25,26} LATS2, an important kinase of the Hippo signaling pathway, has been proven to be a tumor suppressor in liver cancer and lung cancer.^{27,28} Among various signaling pathways, the Hippo-YAP signaling pathway has been identified to be involved in the regulation of multiple tumors.^{29,30} These analyses indicated that the interaction between LATS2 and the Hippo-YAP signaling pathway might underlie the regulatory function of miR-224-3p in the progression of retinoblastoma. Accumulating evidence has suggested that activation of the Hippo-YAP signaling pathway plays an antitumor role in different types of cancer, including gastric cancer, breast cancer, and prostate cancer.³¹⁻³³ The Hippo-YAP signaling pathway plays a critical role in mediating VEGF-induced angiogenesis, where knockdown or inhibition of YAP/TAZ was found to result in a significant decrease in angiogenesis triggered by VEGF.³⁴ In the current study, LATS2 overexpression also led to low expression of VEGF, suggesting that LATS2 over-

expression could suppress angiogenesis. The expression of YAP, TAZ, CYGF, and CYR61 was decreased when LATS2 was overexpressed, which was consistent with the aforementioned research. CCN family proteins including CYR61 and CTGF, which depend on both YAP and TAZ,³⁵ have been identified to play important roles in skeletal growth, wound cure, fibrosis, and cancer.³⁶ Wang et al.³⁷ identified the crucial roles of YAP and TAZ in the regulation of vascular homeostasis. The present study found increased expression of YAP, TAZ, CYGF, and CYR61 in response to miR-224-3p upregulation, indicating that miR-224-3p repressed LATS2 expression and further suppressed the Hippo-YAP signaling pathway, by which miR-224-3p facilitated tumor angiogenesis.

In conclusion, our findings demonstrated that the downregulation of miR-224-3p increases LATS2 and activates the Hippo-YAP signaling pathway, thereby promoting apoptosis, suppressing the proliferation ability of retinoblastoma cells, and restraining tumor growth and angiogenesis. These results led to the understanding that miR-224-3p might potentially be a new promising therapeutic target for retinoblastoma. However, downstream targets of miR-224-3p or other pathways interconnected with the Hippo-YAP signaling pathway that are involved in the pathophysiologic process of retinoblastoma require more extensive investigations in future studies.

Acknowledgments

The authors thank all participants enrolled in the present study.

Disclosure: **L. Song**, None; **Y. Huang**, None; **X. Zhang**, None; **S. Han**, None; **M. Hou**, None; **H. Li**, None

References

- Bremner R, Sage J. Cancer: the origin of human retinoblastoma. *Nature*. 2014;514:312-313.
- Dimaras H, Kimani K, Dimba EA, et al. Retinoblastoma. *Lancet*. 2012;379:1436-1446.
- Dimaras H, Corson TW, Cobrinik D, et al. Retinoblastoma. *Nat Rev Dis Primers*. 2015;1:15021.
- Abramson DH. Retinoblastoma: saving life with vision. *Annu Rev Med*. 2014;65:171-184.
- Benavente CA, Dyer MA. Genetics and epigenetics of human retinoblastoma. *Annu Rev Pathol*. 2015;10:547-562.
- Adlakha YK, Seth P. The expanding horizon of microRNAs in cellular reprogramming. *Prog Neurobiol*. 2017;148:21-39.
- Rupaimoole R, Slack FJ. MicroRNA therapeutics: towards a new era for the management of cancer and other diseases. *Nat Rev Drug Discov*. 2017;16:203-222.
- Liu S, Hu C, Wang Y, Shi G, Li Y, Wu H. miR-124 inhibits proliferation and invasion of human retinoblastoma cells by targeting STAT3. *Oncol Rep*. 2016;36:2398-2404.
- Liu K, Huang J, Xie M, et al. MIR34A regulates autophagy and apoptosis by targeting HMGB1 in the retinoblastoma cell. *Autophagy*. 2014;10:442-452.
- Bai S, Tian B, Li A, Yao Q, Zhang G, Li F. MicroRNA-125b promotes tumor growth and suppresses apoptosis by targeting DRAM2 in retinoblastoma. *Eye (Lond)*. 2016;30:1630-1638.
- Fang W, Shu S, Yongmei L, Endong Z, Lirong Y, Bei S. miR-224-3p inhibits autophagy in cervical cancer cells by targeting FIP200. *Sci Rep*. 2016;6:33229.
- Pu M, Chen J, Tao Z, et al. Regulatory network of miRNA on its target: coordination between transcriptional and post-

- transcriptional regulation of gene expression. *Cell Mol Life Sci*. 2019;76:441–451.
13. Sun Z, Zhang A, Zhang L. Inhibition of microRNA492 attenuates cell proliferation and invasion in retinoblastoma via directly targeting LATS2. *Mol Med Rep*. 2019;19:1965–1971.
 14. Taha Z, Janse van Rensburg HJ, Yang X. The Hippo pathway: immunity and cancer. *Cancers (Basel)*. 2018;10:94
 15. Plouffe SW, Meng Z, Lin KC, et al. Characterization of Hippo pathway components by gene inactivation. *Mol Cell*. 2016;64:993–1008.
 16. Ma Y, Yang Y, Wang F, Wei Q, Qin H. Hippo-YAP signaling pathway: a new paradigm for cancer therapy. *Int J Cancer*. 2015;137:2275–2286.
 17. Kamihara J, Bourdeaut F, Foulkes WD, et al. Retinoblastoma and neuroblastoma predisposition and surveillance. *Clin Cancer Res*. 2017;23:e98e106.
 18. Chen Y, Gao DY, Huang L. In vivo delivery of miRNAs for cancer therapy: challenges and strategies. *Adv Drug Deliv Rev*. 2015;81:128–141.
 19. Gui F, Hong Z, You Z, Wu H, Zhang Y. MiR-21 inhibitor suppressed the progression of retinoblastoma via the modulation of PTEN/PI3K/AKT pathway. *Cell Biol Int*. 2016;40:1294–1302.
 20. Wang Z, Dabrosin C, Yin X, et al. Broad targeting of angiogenesis for cancer prevention and therapy. *Semin Cancer Biol*. 2015;35(suppl):S224–S243.
 21. Wang W, Zhang E, Lin C. MicroRNAs in tumor angiogenesis. *Life Sci*. 2015;136:28–35.
 22. Liu Y, Zhao L, Li D, et al. Microvesicle-delivery miR-150 promotes tumorigenesis by up-regulating VEGF, and the neutralization of miR-150 attenuate tumor development. *Protein Cell*. 2013;4:932–941.
 23. Wei W, Wang Y, Yu X, Ye L, Jiang Y, Cheng Y. Expression of TP53, BCL-2, and VEGFA genes in esophagus carcinoma and its biological significance. *Med Sci Monit*. 2015;21:3016–3022.
 24. Lai YC, Li CC, Sung TC, Chang CW, Lan YJ, Chiang YW. The role of cardiolipin in promoting the membrane pore-forming activity of BAX oligomers. *Biochim Biophys Acta Biomembr*. 2019;1861:268–280.
 25. Chakraborty S, Khare S, Dorairaj SK, Prabhakaran VC, Prakash DR, Kumar A. Identification of genes associated with tumorigenesis of retinoblastoma by microarray analysis. *Genomics*. 2007;90:344–353.
 26. Tschop K, Conery AR, Litovchick L, et al. A kinase shRNA screen links LATS2 and the pRB tumor suppressor. *Genes Dev*. 2011;25:814–830.
 27. Zhang L, Li S, Wang R, Chen C, Ma W, Cai H. Anti-tumor effect of LATS2 on liver cancer death: role of DRP1-mediated mitochondrial division and the Wnt/beta-catenin pathway. *Biomed Pharmacother*. 2019;114:108825.
 28. Xie Y, Lv Y, Zhang Y, Liang Z, Han L, Xie Y. LATS2 promotes apoptosis in non-small cell lung cancer A549 cells via triggering Mff-dependent mitochondrial fission and activating the JNK signaling pathway. *Biomed Pharmacother*. 2019;109:679–689.
 29. Chai Y, Xiang K, Wu Y, et al. Cucurbitacin B inhibits the Hippo-YAP signaling pathway and exerts anticancer activity in colorectal cancer cells. *Med Sci Monit*. 2018;24:9251–9258.
 30. Shi Y, Geng D, Zhang Y, et al. LATS2 inhibits malignant behaviors of glioma cells via inactivating YAP. *J Mol Neurosci*. 2019;68:38–48.
 31. Ye C, Wang W, Xia G, et al. A novel curcumin derivative CL-6 exerts antitumor effect in human gastric cancer cells by inducing apoptosis through Hippo-YAP signaling pathway. *Onco Targets Ther*. 2019;12:2259–2269.
 32. He Z, Zhao TT, Jin F, et al. Downregulation of RASSF6 promotes breast cancer growth and chemoresistance through regulation of Hippo signaling. *Biochem Biophys Res Commun*. 2018;503:2340–2347.
 33. Liu N, Mei L, Fan X, et al. Phosphodiesterase 5/protein kinase G signal governs stemness of prostate cancer stem cells through Hippo pathway. *Cancer Lett*. 2016;378:38–50.
 34. Azad T, Janse van Rensburg HJ, Lightbody ED, et al. A LATS biosensor screen identifies VEGFR as a regulator of the Hippo pathway in angiogenesis. *Nat Commun*. 2018;9:1061.
 35. Futakuchi A, Inoue T, Wei FY, et al. YAP/TAZ are essential for TGF-beta2-mediated conjunctival fibrosis. *Invest Ophthalmol Vis Sci*. 2018;59:3069–3078.
 36. Chen PC, Cheng HC, Yang SF, Lin CW, Tang CH. The CCN family proteins: modulators of bone development and novel targets in bone-associated tumors. *Biomed Res Int*. 2014;2014:437096.
 37. Wang KC, Yeh YT, Nguyen P, et al. Flow-dependent YAP/TAZ activities regulate endothelial phenotypes and atherosclerosis. *Proc Natl Acad Sci U S A*. 2016;113:11525–11530.